JOURNAL OF GEOPHYSICAL RESEARCH, VOL. 102, NO. D14, PAGES 16,959–16,969, JULY 27, 1997

Long-term daily monitoring of Saharan dust load over ocean using Meteosat ISCCP-B2 data 2. Accuracy of the method and validation using Sun photometer measurements

C. Moulin,[1] F. Dulac,[2] C. E. Lambert,[2] P. Chazette,[1] I. Jankowiak,[3] B. Chatenet,[4] and F. Lavenu[5]

Abstract. The accuracy of a method for long-term monitoring of the desert aerosol optical thickness over the oceans using Meteosat low-resolution images, presented in a companion paper, is assessed. We present Sun photometer measurements of aerosol optical thickness and Angström wavelength exponent obtained in 1986-1994 at different sites and seasons in the tropical Atlantic and northwestern Mediterranean. Results suggest that in the absence of dust outbreak the optical effects of the marine aerosol are dominated by continental anthropogenic sulphates in the Mediterranean Sea and by continental desert dust in the tropical Atlantic. We rely on this data set to constrain the desert aerosol model used in the Meteosat data inversion. We obtain the best agreement between Meteosat- and Sun-photometer-derived aerosol optical thickness with a size distribution typical of background desert aerosol and a refractive index of 1.50 - *i* 0.010. The main theoretical uncertainties on the desert aerosol optical thickness estimated from Meteosat are due to the sensor calibration and to the radiometric sensitivity. Comparison of Meteosat-derived estimates of the desert aerosol optical thickness with independent Sun photometer measurements exhibits a maximum dispersion of 25%.

1. Introduction

In part 1 of this paper [*Moulin et al.*, this issue] we describe a method to monitor African dust optical thickness and mass column density from multiannual time series of Meteosat images, using the radiative transfer model of *Tanré et al.* [1990] and appropriate aerosol models. We use one daily degraded image (ISCCP-B2 format) from the Meteosat VIS solar wide band (0.35-1.1 μm), to limit the computer time and memory requirements. Sun photometer measurements of atmospheric aerosol optical thickness are particularly appropriate to test and validate the satellite determinations [*Jankowiak and Tanré*, 1992; *Ignatov et al.*, 1995]. Indeed, such data are suitable as a reference for comparison because the aerosol optical thickness is directly derived from the measured attenuation of the solar irradiance during its path through the atmosphere, without any hypothesis on aerosol optical properties, contrary to satellite inversion methods.

In this paper we use Sun photometer spectral measurements to test and validate our Meteosat inversion procedure. We first present Sun photometer measurements and discuss the relevant results (aerosol optical thickness at 0.55 μm and Angström exponent in the visible) derived from these measurements. We then use a first subset of data corresponding to desert dust occurrences to constrain the dust aerosol model used for the Meteosat data inversion and a second independent set of data to validate the inversion. Finally, we estimate the uncertainty of our determination of the local dust optical thickness, and we illustrate the validity and limits of using interpolation to estimate the dust optical thickness in cloudy areas.

2. Sun Photometer Data

2.1. Measurements and Instrumentation

We report here solar spectral transmission measurements that we performed during several campaigns in the Mediterranean and northeastern Atlantic, and we also use the measurements from coastal Senegal reported by *Jankowiak and Tanré* [1992]. Table 1 gives an overview of the stations, measurement periods, and data. All measurements have been done with a portable radiometer developed in 1985 at the Laboratoire de Météorologie Dynamique, Palaiseau, France, following a prototype from the Laboratoire d'Optique Atmosphérique, Lille, France [*Tanré et al.*, 1988]. The instrument had an angular field of view of 3° and was equipped with three aerosol channels at 0.449, 0.648, and 0.845 μm, with bandwidths of less than 20 nm. Two other near-infrared channels allowed the retrieval of the total atmospheric water vapor content. Only the measurements in the visible part of the spectrum are considered here, as the Meteosat-derived aerosol optical thickness is at 0.550 μm. By means of the usual Langley plot method the instrument was calibrated by measurements in altitude (2862 m) at the Observatoire du Pic du Midi de Bigorre, in the French Pyrenees,

[1]Laboratoire de Modélisation du Climat et de l'Environnement, Direction des Sciences de la Matière, Commissariat à l'Energie Atomique, Gif-Sur-Yvette, France.
[2]Centre des Faibles Radioactivités Centre de la Recherche Scientifique, Gif-Sur-Yvette, France.
[3]Laboratoire d'Optique Atmosphérique, Université des Sciences et Techniques de Lille- CNRS, Villeneuve d'Ascq, France.
[4]Laboratoire Interuniversitaire des Sytèmes Atmosphériques, Universités de Paris 7, Paris 12- CNRS, Créteil, France.
[5]Institute Français de Recherche Scientifique pour le Développement en Coopération, Ouagadougou, Burkina Faso.

Paper number 96JD02598.
0148-0227/97/96JD-02598$09.00

Long-term daily monitoring of Saharan dust load over marine areas using Meteosat ISCCP-B2 data. Part II: Accuracy of the method and validation using sunphotometer measurements

C. MOULIN,[1] F. DULAC,[2] C. E. LAMBERT,[2] P. CHAZETTE[1]
I. JANKOWIAK,[3] B. CHATENET,[4] F. LAVENU,[5]

Institut Pierre Simon Laplace
[1]Laboratoire de Modélisation du Climat et de l'Environnement,
Direction des Sciences de la Matière, Commissariat à l'Energie Atomique, Gif-Sur-Yvette, France
and
[2]Centre des Faibles Radioactivités, CNRS - CEA, Gif-Sur-Yvette, France

[3]Laboratoire d'Optique Atmosphérique,
Université des Sciences et Techniques de Lille - CNRS, Villeneuve d'Ascq, France

[4]Laboratoire Interuniversitaire des Sytèmes Atmosphériques
Universités de Paris VII & Paris XII - CNRS, Créteil, France

[5]ORSTOM, BP 182, Ouagadougou, Burkina Faso

Abstract. The accuracy of a method for long term monitoring of the desert aerosol optical thickness over the oceans using Meteosat low resolution images, presented in part I, is assessed. We present sunphotometer measurements of aerosol optical thickness and Angström wavelength exponent obtained in 1986-1994 for different sites and seasons in the tropical Atlantic and northwestern Mediterranean. This data set helps constraining the desert aerosol model used in the Meteosat data inversion. We obtain the best agreement between Meteosat- and sunphotometer-derived aerosol optical thickness with a size distribution typical of background desert aerosol and a refractive index of 1.50-i0.01. The overall theoretical uncertainty of the method on the desert aerosol optical thickness is due to the sensor calibration, the radiometric sensitivity, the aerosol model and the radiative transfer model. It varies between ± 25% and ± 43%, the best values beeing reached for the most recent sensors. The comparison of Meteosat-derived estimates of the desert aerosol optical thickness with sunphotometer measurements exhibits a maximum dispersion of 25%, with an average ratio of 1.

For submission to J.G.R. (accepté)

19/02/96

1. Introduction

Guillard *et al.*, in part I of this paper, describe a method to monitor African dust optical thickness and mass column density from multi-annual time series of Meteosat images, using the radiative transfer model of Tanré *et al.* (1990) and appropriate aerosol models. They use degraded images (ISCCP-B2 format) from the Meteosat VIS solar wide band, in order to limit the computer-time and memory requirements. Sunphotometer measurements of atmospheric aerosol optical thickness are particularly appropriate to test and validate the satellite determinations (Jankowiak and Tanré, 1992; Ignatov *et al.*, 1995). Indeed such data are suitable as a reference for comparison because the aerosol optical thickness is directly derived from the measured attenuation of the solar irradiance during its path through the atmosphere, without any hypothesis on aerosol optical properties, contrary to satellite inversion methods.

In this paper, we use sunphotometer spectral measurements to test and validate our Meteosat inversion procedure. We first present and discuss the sunphotometer measurements (aerosol optical thickness at 0.55 μm and Angström wavelength exponent). We then use a first subset of data corresponding to desert dust occurrences to constrain the dust aerosol model used for the Meteosat data inversion, and a second independant set of data to validate the inversion. Finally, we estimate the uncertainty of our determination of the local dust optical thickness, and we illustrate the interest and limits of using interpolation to estimate the dust optical thickness in cloudy areas.

2. Sunphotometer data

2.1 Measurements and instrumentation

We report here solar spectral transmission measurements performed during several campaigns in the Mediterranean and northeastern Atlantic, and we also use in the following measurements from coastal Senegal reported by Jankowiak and Tanré (1992). **Table 1** gives an overview of the stations, measurements periods and data. All measurements have been done with a portable radiometer developped in 1985 at the Laboratoire de Météorologie Dynamique, Palaiseau, France, following a prototype from the Laboratoire d'Optique Atmosphérique, Lille, France (Tanré *et al.*, 1988). The instrument had an angular field of view of 3° and was equipped with three aerosol channels at 0.449, 0.648 and 0.845 μm, with bandwidths of less than 20 nm. Two other near-infrared channels allowed the retrieval of the total atmospheric water vapor content. Only the measurements in the visible part of the spectrum are considered here, as the Meteosat-derived aerosol optical thickness is at 0.550 μm. By means of a Langley plot method, the instrument was calibrated by measurements in altitude (2862 m) at the Observatoire du Pic du Midi

de Bigorre, in the French Pyrenees, in December 1985, and the calibration was monitored during the campaigns. Comparisons with a standard reference radiometer were performed in Lille between the different campaigns, and the filter transmission bands were checked to be identical to the original after five years.

Since late October 1994, an automated suntracking photometer, model CE318, manufactured by CIMEL Electronique, Paris, has been installed and routinely operated at the meteorological rawindsounding station of Sal Island. Data are transmitted in real time via Meteosat. The instrument field of view is 1° and the two aerosol channels of interest are at wavelengths of 0.449 and 0.667 μm (Holben *et al.*, in press).

A few from all measurements were rejected, when replicate measurements revealed inconsistent results. This data set of 107 days with measurements of the spectral aerosol optical thickness has the advantages that: (i) it covers a large part of the 12-year period of Meteosat ISCCP archive; (ii) it includes coherent measurements performed at different places and seasons in the Atlantic and the Mediterranean: measurements were made at the same time as our Meteosat analyses (about 11:45 TU), as well as measurements at different hours in a given day; (iii) it covers a wide range of atmospheric conditions, from very clear background atmospheres to very turbid atmospheres. Therefore, this data set should enable us to test and validate the inversion method for a wide range of dust optical thicknesses, using sensors with both a poor (Meteosat-2) or an improved (Meteosat-4 and -5) radiometric sensitivity, and within a wide range of geometric conditions.

2.2 Sunphotometer data processing

Aerosol optical thickness. The total optical thickness of the atmosphere at wavelength λ, τ_λ, is calculated using:

$$E_\lambda = E_\lambda^0 \exp\left(-\frac{\tau_\lambda}{\mu_0}\right) \qquad (1)$$

where E_λ and E_λ^0 are the solar irradiance respectively at the ground and at the satellite level and μ_0 the cosine of the solar zenith angle, or the inverse of the relative optical air mass. The total atmospheric optical thickness results from Rayleigh and aerosol scattering, as well as from gaseous absorption in the stratosphere:

$$\tau_\lambda = \tau_\lambda^R + \tau_\lambda^A + \tau_\lambda^G \qquad (2)$$

where τ_λ^R and τ_λ^A are respectively the Rayleigh and aerosol optical thicknesses and τ_λ^G the absorbing gases optical thickness. τ_λ^A is deduced from equation 2 by calculating τ_λ^R and τ_λ^G. τ_λ^R

directly depends on the atmospheric pressure, which was also measured, and τ_λ^G is related to the atmospheric gaseous transmission, T_λ^G, by:

$$\tau_\lambda^G = -\mu_0 \log(T_\lambda^G) \tag{3}$$

Some ozone absorption occurs in the spectral transmission band of the 0.650 μm filter. The ozone optical thickness was derived from mean climatological values for a standard tropical or mid-latitude atmosphere (Mc Clatchey *et al.*, 1971), respectively for Atlantic and Mediterranean measurements. The aerosol optical thickness are retrieved within ±5% (Tanré et al, 1988).

Angström spectral exponent. The aerosol optical thickness at 0.550 μm was derived from the measurements in the blue and red channels using the well-known spectral dependance of the aerosol optical thickness in the visible (Angström, 1964):

$$\frac{\tau_{\lambda_1}^A}{\tau_{\lambda_2}^A} = \left(\frac{\lambda_1}{\lambda_2}\right)^{-\alpha} \tag{4}$$

where the Angström exponent, α, may be directly related to the aerosol size distribution (Junge, 1963). Uncertainties of ±5% on the aerosol optical thickness at the two wavelengths result in an uncertainty on α generally comprised between 8 and 15%. Small or even negative values are found for large particles such as seasalts or desert dust aerosols, whereas values between 1.5 and 2 are found for small particles such as sulphates (Laulainen *et al.*, 1978; Guillard *et al.*, this issue). The extreme value of 4 corresponds to pure Rayleigh scattering by non absorbing molecules. In background marine conditions with a mixture of large seasalt and small sulphate particles, Tomasi and Prodi (1982) and Hoppel *et al.* (1990) measured mean Angström exponent values of 0.6 and 0.8 respectively for the remote marine atmosphere, and they attributed its variability (from 0.4 to 1.5) to the sea salt contribution. Indeed, seasalt particles, produced by the wind, are large and have then a slightly negative Angström exponent of - 0.10 (Guillard *et al.*, this issue) which decreases the average value of the mixture. Numerous works showed that when desert dust particles are present, the Angström exponent generally ranges between 0 and 0.5 both over Africa (Fouquart *et al.*, 1987; Holben *et al.*, 1991; Ben Mohamed *et al.*, 1992) and over marine remote regions (Carlson and Caverly, 1977; Tomasi *et al.*, 1979).

2.3 Results

The results obtained at M'bour have been used previously by Jankowiak and Tanré (1992) to validate Meteosat-2 desert aerosol inversions. The optical thicknesses measured in April 1987 were particularly large, with values ranging between 0.62 and 2.25, due to the occurrence of

Table 1. Summary of Solar Spectral Transmission Measurements Used in This Work

Location	Period	Instrument Type
Capo Cavallo, NW coast of Corsica (42.52°N, 8.67°E)	March 22 to April 22, 1986 (12 days)	portable radiometer [a]
M'bour, coastal Senegal (14.40°N, 17.00°W)	April 1 to May 3, 1987 (12 days)	portable radiometer [a]
NE tropical Atlantic, R/V *L'Atalante* (15.50°-27.70°N, 17.90°-31.15°W)	September 14-29, 1991 (15 days)	portable radiometer [a]
Sal Island, Cape Verde (16.73°N, 22.95°W)	December 4-12, 1991 (8 days)	portable radiometer [a]
Sal Island, Cape Verde (16.73°N, 22.95°W)	May 22-27, 1992 (4 days)	portable radiometer [a]
Sal Island, Cape Verde (16.73°N, 22.95°W)	October 22 to December 30, 1994 (56 days)	automatic scanning photometer [b]

[a] *Tanré et al.* [1988]; *Liousse et al.* [1995].
[b] *Holben et al.* [1996].

in December 1985, and the calibration was monitored during the campaigns, using the same method. Comparisons with a standard reference radiometer were performed in Lille between the different campaigns, and the filter transmission bands were checked to be identical to the original after 5 years.

Since late October 1994, an automated Sun-tracking photometer, model CE318, manufactured by CIMEL Electronique, Paris, has been installed and routinely operated on top of the 8-m-high building of the meteorological rawind sounding station of Sal Island. Data are transmitted in quasi real time via Meteosat. The instrument field of view is 1° and the two aerosol channels of interest are at wavelengths of 0.449 and 0.667 μm [*Holben et al.*, 1996].

A few from all measurements were rejected when replicate measurements revealed inconsistent results. The data set obtained contains 107 days of measurements of the spectral aerosol optical thickness and has the advantages that (1) it covers a large part of the 12-year period of Meteosat ISCCP archive; (2) it includes coherent measurements performed at different places and seasons in the Atlantic and the Mediterranean; (3) measurements were generally made at the same time as our Meteosat analyses (about 1145 UT) as well as at different hours in a given day; (4) it covers a wide range of atmospheric conditions, from very clear background atmospheres to very turbid atmospheres. Therefore this data set should enable us to test and validate the inversion method for a wide range of dust optical thicknesses, using sensors with both a poor (Meteosat 2) or an improved (Meteosat 4 and 5) radiometric sensitivity and within a wide range of geometric conditions.

2.2. Sun Photometer Data Processing

Aerosol optical thickness. The total optical thickness of the atmosphere at wavelength λ, τ_λ is calculated using the Beer-Lambert law, assuming that the contribution of multiple scattering within the field of view of the Sun photometer is negligible:

$$E_\lambda = E_\lambda^S \exp\left(-\frac{\tau_\lambda}{\mu_S}\right) \tag{1}$$

where E_λ and E_λ^s are the solar irradiances at the ground and at the satellite level, respectively and μ_S is the cosine of the solar zenith angle, or the inverse of the relative optical air mass. The total atmospheric optical thickness results from Rayleigh and aerosol scattering as well as from gaseous absorption in the stratosphere:

$$\tau_\lambda = \tau_\lambda^R + \tau_\lambda^A + \tau_\lambda^g \tag{2}$$

where τ_λ^R and τ_λ^A are the Rayleigh and aerosol optical thicknesses, respectively, and τ_λ^g is the optical thickness of absorbing gases. The parameter τ_λ^A is deduced from equation (2) by calculating τ_λ^R and τ_λ^g. The parameter τ_λ^R directly depends on the atmospheric pressure, which was also measured, and τ_λ^g is related to the atmospheric gaseous transmission T_λ^g by

$$\tau_\lambda^g = -\mu_S \log(T_\lambda^g) \tag{3}$$

Some ozone absorption occurs in the spectral transmission band of the 0.648-μm filter. The ozone optical thickness was derived from mean climatological values for a standard tropical or midlatitude atmosphere [*Mc Clatchey et al.*, 1971] for Atlantic and Mediterranean measurements, respectively.

Angström exponent. The aerosol optical thickness at 0.550 μm was derived from the measurements in the blue and red channels using the following relation, derived from the well-known spectral dependence of the aerosol optical thickness in the visible spectrum [*Angström*, 1964]:

$$\frac{\tau_{\lambda_1}^A}{\tau_{\lambda_2}^A} = \left(\frac{\lambda_1}{\lambda_2}\right)^{-\alpha} \tag{4}$$

where the Angström exponent α is related to the aerosol size distribution [*Junge*, 1963]. Typical uncertainties on the aerosol optical thickness at visible wavelengths (±5% for $\tau_{0.55}^A = 0.4$ [*Fouquart et al.*, 1987; *Tanré et al.*, 1988]) result in an uncertainty on α, which generally ranges from 8 to 15%, but much larger relative uncertainties may occur for small values of $\tau_{0.55}^A$. Small or even negative values of α are found for large particles such as sea salts or desert dust aerosols, whereas values between 1.5 and 2 are found for small particles such as sulphates [*Lauleinen et al.*, 1978; *Moulin et al.*, this issue]. The extreme value of 4 corresponds to pure Rayleigh scattering. In background marine conditions with a mixture of large sea-salt and small sulphate particles, *Tomasi and Prodi* [1982] and *Hoppel et al.* [1990] measured mean Angström exponent values of 0.6 and 0.8, respectively, for the remote marine atmosphere, and they attributed its variability (from 0.4 to 1.5) to the sea-salt

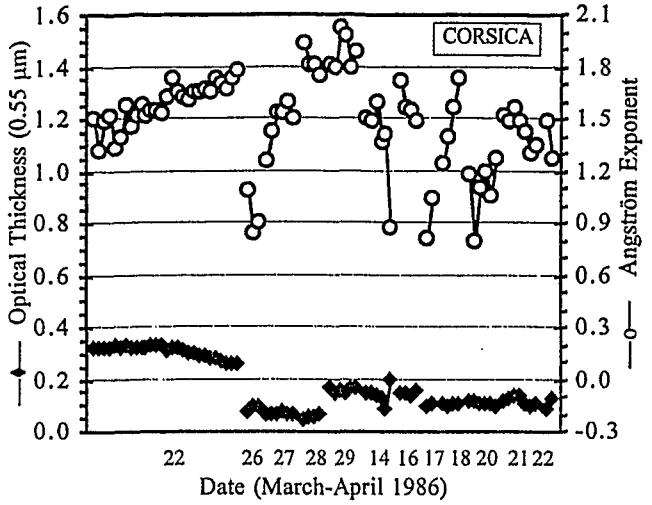

Figure 1. Sequential results of aerosol optical thickness at 0.55 µm and Angström exponent (from blue and red channels) during the measurement campaign in Corsica.

contribution. Indeed, the slightly negative Angström exponent of large sea-salt particles produced by the wind (-0.1 [*Moulin et al.*, this issue]) tends to decrease the average value of the sea salt and sulphate mixture. Numerous works showed that when desert dust particles are present, the Angström exponent generally ranges between 0 and 0.5 both over Africa [*Fouquart et al.*, 1987; *Holben et al.*, 1991; *Ben Mohamed et al.*, 1992] and over marine remote regions [*Carlson and Caverly*, 1977; *Tomasi et al.*, 1979].

2.3. Results

The results obtained at M'bour have been used previously by *Jankowiak and Tanré* [1992] to validate Meteosat 2 desert aerosol inversions. The optical thicknesses measured in April 1987 were particularly large, with values ranging between 0.62 and 2.25, due to the occurrence of dust outbreaks, particularly frequent at this period of the year [*D'Almeida*, 1987; *Jankowiak and Tanré*, 1992]. Our own set of results of $\tau_{0.55}^{A}$ and α from Sun photometer measurements are presented in Figures 1 to 4.

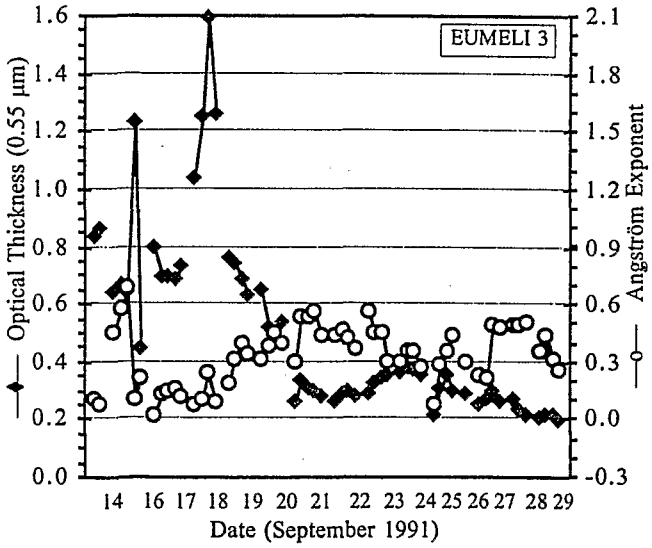

Figure 2. As in Figure 1 but for the third eutrophe-mesotrophe-oligotrophe (EUMELI 3) measurement campaign.

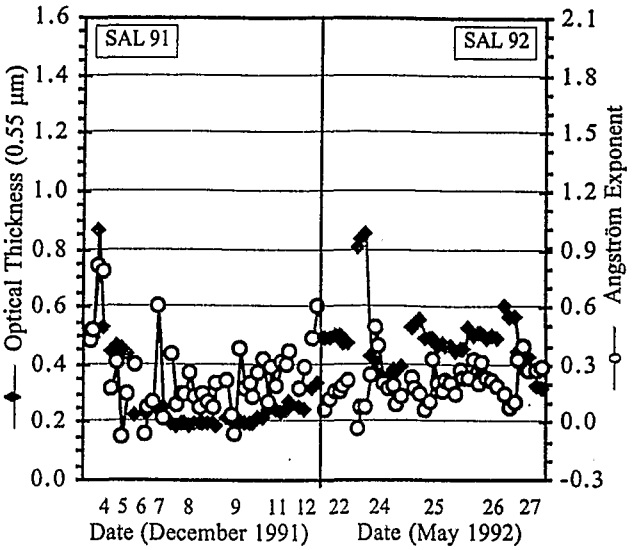

Figure 3. As in Figure 1 but for the measurement campaigns of December 1991 and May 1992 at Sal Island.

Measurements from Corsica in spring 1986, shown in Figure 1, have been mentioned by *Dulac et al.* [1992a]. They were performed at an aerosol-monitoring station operated between 1985 and 1988 [*Bergametti et al.*, 1989] during typical nondust conditions of the northwestern Mediterranean. A high-pollution episode with a peak of excess sulphur concentration occurred on March 22 with air mass trajectories from the north [*Bergametti*, 1987] and was responsible for the relatively large value of $\tau_{0.55}^{A}$ (0.25 - 0.30). Apart from this event the aerosol optical thickness measured in Corsica remained low during the observations (0.05-0.19). The Angström exponents during the pollution event are characteristic of sulphates (around 1.5), but all along the measurement period, they were larger than 0.8 and remained typical of an aerosol rich in submicronic sulphates. The Angström exponent exhibits stronger variations than the aerosol optical thickness, mainly because it is more sensitive to the presence of large particles (sea-salt).

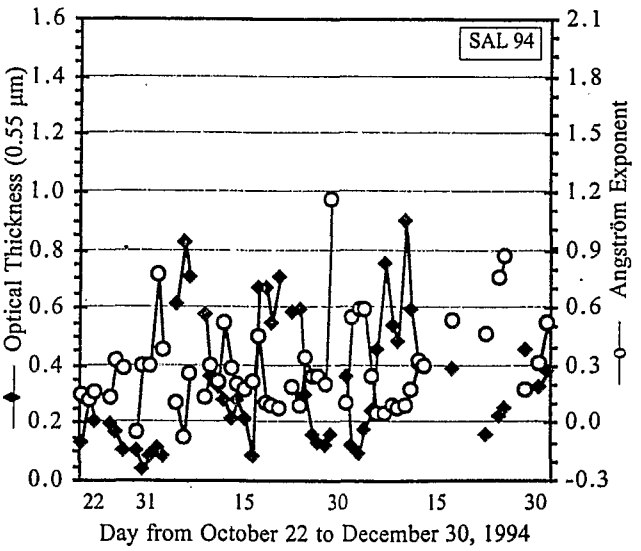

Figure 4. As in Figure 1 but for the measurement campaign with the automatic scanning photometer at Sal Island, in late, 1994. Only the closest observation to 1145 UT is shown per day.

Figure 2 shows data from the northeastern subtropical Atlantic collected in September 1991 onboard the French R/V *L'Atalante* during the third eutrophe-mesotrophe-oligotrophe (EUMELI 3) oceanographic cruise, a few months after the eruption of Mount Pinatubo in summer 1991 which resulted in exceptionally high stratospheric aerosol optical thicknesses (of the order of 0.2 at these latitudes [*Jäger* et al., 1995]). A dust outbreak and marine background conditions were encountered during this cruise [*Putaud et al.*, 1993], but much smaller Angström exponents ($\alpha <$ 0.8) were found than in Corsica. The smallest values ($\alpha < 0.3$) were generally associated with the largest aerosol optical thicknesses (up to more than 1) due to a dust plume at the beginning of the cruise. During the second part of the cruise, aerosol optical thicknesses remained lower than 0.4, implying that there was no dust event, but a relatively low Angström exponent (0.2 - 0.6) suggests the presence of large particles in the background aerosol.

Figure 3 illustrates measurements performed at Sal Island at an aerosol-monitoring station operated since December 1991 [*Chiapello et al.*, 1995]. Measurements made in December 1991 and May 1992 occurred in the absence of any dust outbreak but were influenced by stratospheric aerosols from Mount Pinatubo. We experienced rains and unusual easterly winds in December 1991, and particularly low aerosol concentrations were observed between December 6 and 12, 1991 [*Chiapello et al.*, 1995]. In December 1991 the baseline aerosol optical thickness is of 0.2, and somewhat larger values of $\tau^A_{0.55}$ were observed at Sal in May 1992. During these two campaigns the low Angström exponent values (0 - 0.4) reveal, as for the EUMELI 3 campaign, the presence of large particles in the background marine aerosol.

In Figure 4 the series of automated measurements performed at Sal from late October to early December 1994 show three important peaks of aerosol optical thicknesses with values larger than 0.5 during several days, separated by periods of lower values (down to 0.05). These peaks in $\tau^A_{0.55}$ correspond to particularly small values of the Angström exponent ($\alpha < 0.1$), whereas during background marine conditions, it typically ranges between 0.2 and 0.6, as for the previous campaigns in the Atlantic.

Very different Angström exponents are found in the northwestern Mediterranean and tropical Atlantic. In the Mediterranean (Figure 1) the background aerosol has an Angström exponent comparable to the range found during a high-pollution episode, which suggests that secondary sulphates from European anthropogenic pollution sources might dominate the background aerosol. In the Atlantic the Angström exponent observed (Figures 2, 3, and 4) appears lower than 0.6 even in the case of low-aerosol optical thickness (0.1 or less, i.e., comparable to background values observed in the Mediterranean), which suggests that the background aerosol in the tropical Atlantic is influenced by large particles, possibly African dust. Figures 1 to 4 also show that $\tau^A_{0.55}$ and α generally have opposite variations, which implies that the magnitude of $\tau^A_{0.55}$ is mainly controlled by the presence of large particles.

For comparison between coincident Sun-photometer-derived and Meteosat-derived aerosol optical thickness, we selected measurements representative of African dust. We retained only Sun photometer data when measurements were done between 1115 and 1215 UT, because Meteosat slot 24 images are taken between 1130 and 1155 UT, and when α was lower than or equal to 0.5 in order to eliminate the nondust conditions. This last criterion eliminates all measurements performed in Corsica in March - April 1986. This subset has been further divided into two groups used separately. The first group (from 1987 to 1991) of manual measurements was used in a first step to constrain the Meteosat data inversion via the parameters of the dust aerosol model, whereas the second group (from 1994) of automated measurements was then used independently for the validation of the inversion.

3. Constraints on the Desert Aerosol Model

In this section, we used the first part of our Sun photometer subset of data (data before 1994) to constrain the characteristics of the dust aerosol model used during our Meteosat data inversion. A complete description of the Meteosat inversion method is given in part 1 [*Moulin et al.*, this issue].

3.1. Comparison Between Meteosat and Sun Photometer Measurements

The strong difference between Meteosat and Sun photometer technologies yields some uncertainties when comparing the two data sets. Indeed, Meteosat has a wide field of view and a wide spectral band compared to the Sun photometer. Meteosat measurement also includes two paths through the atmosphere instead of one for the photometer. Thus Meteosat is sensitive to surface reflectance and to aerosol scattering, contrary to the Sun photometer measurement, which is sensitive to solar extinction. However, Sun photometers give a direct measurement of attenuation, and therefore Sun-photometer-derived aerosol optical thicknesses were considered as the reference "ground truth" data set for our comparison purpose.

The scattering angles of Meteosat measurements corresponding to our Sun photometer measurements vary between 160° and 177° and thus cover a large part of the total range encountered for the Meteosat observations over the Mediterranean and the Atlantic (150°-180° [*Moulin et al.*, this issue]). For this first analysis the Meteosat inversion was performed using the background desert aerosol size distribution model defined by *Shettle* [1984] and a complex refractive index of 1.55 - *i* 0.005, constant over the whole Meteosat spectral band, in agreement with measurements of African dust over the Atlantic [*Patterson et al.*, 1977]. The size distribution of *Shettle* [1984] has already been used for dust optical thickness determination from Meteosat data analysis [*Jankowiak and Tanré*, 1992; *Dulac et al.*, 1992a] and was found compatible with observed desert dust size distributions. For instance, *Dulac et al.* [1989, 1992a] measured, using cascade impactors in Corsica and in the Mediterranean, a mass median diameter close to the second mode of *Shettle* [1984]. Moreover, from total deposition measurements they estimated a mean deposition velocity of desert dust in agreement with the sedimentation velocity calculated by using *Shettle*'s [1984] particle size distribution model. In addition, the use of the *Shettle's* [1984] model for long-range transport modeling of Saharan dust yielded dust optical thickness values consistent with Meteosat measurements over the Mediterranean and Atlantic when the model results were found very sensitive to the dust particle size distribution [*Balkanski et al.*, 1996]. The Meteosat-derived optical thicknesses compared to the reference values were averaged within a square of 3 × 3 pixels, i.e., a zone of about 100 km × 100 km. This zone was taken as close as possible to the Sun photometer measurement location, and for coastal sites the zone was shifted from one pixel off-shore (about 30 km) to avoid contamination by the high reflectances of lands or turbid waters

[*Moulin et al.*, this issue]. Among the total of 40 days of measurements available from the first subset of data, only 24 allowed a comparison, because in some cases the nine Meteosat pixels had been filtered out by our cloud detection tests or because of aerosol optical thickness lower than Meteosat detection limit. The selected Sun photometer data used for comparison with Meteosat-derived $\tau^A_{0.55}$ are presented in Table 2, including the date and location as well as the aerosol optical thickness and Angström exponent of each measurement. The comparison between Sun-photometer-retrieved and Meteosat-retrieved optical thicknesses showed a good correlation, but the Meteosat-retrieved optical thickness was systematically underestimated by about 40%.

3.2. Discussion

Possible causes of discrepancy. Such a discrepancy between Meteosat and Sun photometer measurements may be due to various causes: an error on the calibration coefficient of the imager, on the sea surface and molecular atmosphere reflectances, on the stratospheric or marine optical thickness, or on the desert aerosol optical properties. Errors on the stratospheric and marine aerosol corrections as well as on the sea surface or molecular atmosphere reflectances would have a stronger impact on Meteosat results for low-aerosol optical thicknesses and thus would lead to an offset rather than a proportional bias on $\tau^A_{0.55}$. As shown by *Moulin et al.* [this issue], the aerosol optical thickness $\tau^A_{0.55}$ retrieved from Meteosat numeric count (NC) depends in first approximation on the Meteosat calibration coefficient and offset, a and NC_0, and on the aerosol optical properties:

$$\tau^A_{0.55} \propto \frac{a\,(NC - NC_0)}{<\omega^A\, P^A(\chi)>} \tag{5}$$

where $<\omega^A\, P^A(\chi)>$ represents the mean scattering efficiency of the aerosol model over the Meteosat spectral band for a given scattering angle χ, ω^A and P^A being the single-scattering albedo and the phase function of the aerosol model, respectively. Calibration coefficients and desert aerosol optical properties may then be suspected to induce such a bias of 40% on the Meteosat-derived aerosol optical thicknesses. The intercalibration procedure developed by *Moulin et al.* [1996] is based on the calibration performed by *Koepke* [1983] for Meteosat 2, and an error in this calibration will directly influence the calibration of the other sensors. *Koepke* [1983] gives an uncertainty of ±10%, and the overall uncertainty on the calibration coefficients used here was estimated to be ±13% [*Moulin et al.*, 1996]. This is too small to account for the bias on Meteosat-derived optical thickness, which is observed for Sun photometer $\tau^A_{0.55}$ ranging from 0.19 to more than 1 (see Table 2). Moreover, we observed that this systematic difference between Sun photometer and Meteosat was the same for Meteosat 2 and 4. Calibration as the source of error is thus unlikely. Therefore only desert aerosol

Table 2. Set of Sun Photometer Measurements Used for Constraining the Refractive Index of the Desert Aerosol Model

Location	Geographical Coordinates	Date	$\tau^A_{0.55}$	α
M'bour, Senegal	14.40°N, 17.00°W	April 1, 1987	1.20	0.01
		April 3, 1987	1.30	0.06
		April 6, 1987	1.09	0.11
		April 8, 1987	0.64	0.13
		April 12, 1987 [a]	0.62	...
		April 16, 1987	1.15	0.25
		April 17, 1987	2.25	-0.09
		April 23, 1987	1.65	0.16
EUMELI 3, North Atlantic	15.50°N, 18.00°W	September 14, 1991	0.83	0.10
	18.50°N, 21.10°W	September 17, 1991	0.69	0.14
	18.50°N, 21.10°W	September 18, 1991	1.25	0.11
	20.65°N, 29.80°W	September 20, 1991	0.65	0.31
	21.05°N, 31.15°W	September 21, 1991	0.32	0.49
	21.05°N, 31.15°W	September 22, 1991	0.29	0.46
	21.05°N, 31.15°W	September 23, 1991	0.32	0.45
	21.05°N, 31.15°W	September 24, 1991	0.36	0.33
	21.05°N, 31.15°W	September 25, 1991	0.30	0.29
	22.70°N, 27.10°W	September 26, 1991	0.29	0.30
	24.55°N, 22.90°W	September 27, 1991	0.26	0.22
	26.00°N, 20.45°W	September 28, 1991	0.27	0.48
	27.70°N, 17.90°W	September 29, 1991	0.21	0.44
Sal Island, Cape Verde	16.73°N, 22.95°W	December 7, 1991	0.24	0.11
		December 8, 1991	0.19	0.10
		December 9, 1991	0.20	0.17

The corresponding Meteosat sensors are Meteosat 2 in 1987 and Meteosat 4 in 1991. The parameter $\tau^A_{0.55}$ is the aerosol optical thickness at 0.550 μm, and α is the Angström exponent computed between 0.449 and 0.648 μm.

[a] Angström exponent not available for this date.

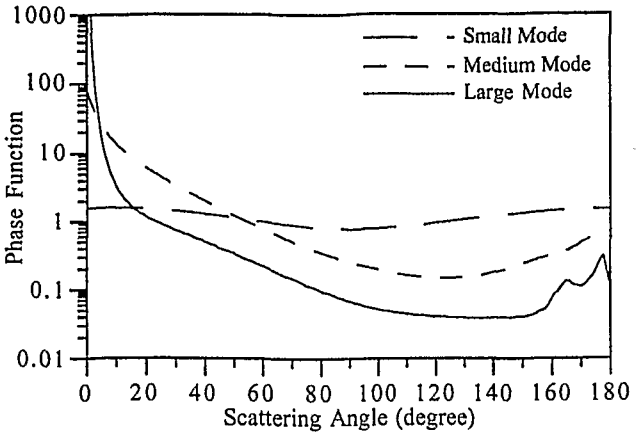

Figure 5. Phase function at $\bar{\lambda}$ = 0.70 μm of the three independent modes of the background desert aerosol model of *Shettle* [1984], as described in Table 3.

optical properties and, particularly, the phase function may be the cause of the discrepancy between Sun-photometer-derived and Meteosat-derived aerosol optical thickness. It is obvious that the lack of knowledge of the actual aerosol characteristics may be a strong source of error. In the following we test the parameters of the desert aerosol model which may cause a variation of the phase function, i.e., the particle size distribution and complex refractive index.

Size distribution. Although the dust size distribution model [*Shettle*, 1984] seems realistic, we have to take into account that the aerosol phase function is particularly sensitive to the particle size distribution for scattering angles above 150°, decreasing when the particle size increases. Figure 5 shows the phase functions of the three modes of the desert background model of *Shettle* [1984]. The first (fine) mode has a phase function characteristic of very small particles, with a quasi-isotropic scattering. For modes 2 (coarse) and 3 (giant) the forward scattering increases with particle size, inducing a general decrease at the other angles. The resulting phase function $P_\lambda^A(\chi)$ for the *Shettle*'s [1984] model is very close to the phase function of the intermediate mode. The equivalent phase function is computed as a weighted average of the phase function P_λ^{Ai} of each mode i as

$$P_\lambda^A(\chi) = \frac{\sum_{i=1}^{3} n_i P_\lambda^{A_i}(\chi) K_\lambda^{sca_i}}{\sum_{i=1}^{3} n_i K_\lambda^{sca_i}} \quad (6)$$

where n_i and $K_\lambda^{sca_i}$ are the proportion in number and the scattering coefficients of mode i, respectively. In fact, only the second mode of this distribution has a significant effect on P_λ^A. Indeed, the scattering coefficient of the fine mode, which accounts for about half of the particle number, is very low and its contribution to the equivalent phase function is negligible, whereas the number of particles in the giant mode is too small to affect the average phase function. A decrease of 30% of the equivalent phase function can only be obtained by increasing by an order of magnitude the number of large particles in the giant mode. In this way the total particle mass would be controlled by the giant mode of the distribution. Such a distribution appears contradictory to existing observations and would induce unrealistic desert dust loads.

In a second step we tested different desert aerosol models from the litterature, presented in Table 3. The trimodal models of *Shettle* [1984] and *D'Almeida* [1987] have been derived from measurements in various arid regions of Africa. The background desert (DD and BD) dust models are representative of transported particles, whereas the wind-carrying (WC) dust model is characteristic of particles near the source. The three monomodal models (D0, D2, and D5) have been computed by *Koepke and Hess* [1988] after loess particle size distribution analyzes by *Schütz* [1980]. They are supposed to be representative of the desert dust aerosol at different times during its transport. The

Table 3. Description of Various Desert Dust Aerosol Models Tested in This Study

	Desert Dust (DD)	Background Dust (BD)	Wind-Carrying Dust (WC)	Dust at Source (D0)	Dust at 2000 km (D2)	Dust at 5000 km (D5)	Dust in Mediterranean (DM1)	Dust in Mediterranean (DM2)
Reference	*Shettle* [1984]	*D'Almeida* [1987]	*D'Almeida* [1987]	*Schütz* [1979]	*Schütz* [1979]	*Schütz* [1979]	*Dulac et al.* [1992a]	*Dulac et al.* [1992b]
Mean diameters, μm	0.0020 0.0436 12.4800	0.16 1.40 10.00	0.104 3.000 24.000	0.31	0.3	0.28	0.59	0.473 4.177
Geometric standard deviations	2.13 3.20 1.89	2.10 1.90 1.60	2.15 2.07 1.70	4	3	2.4	2	2.00 1.85
Number proportions, %	54.21 45.79 3.9×10^{-5}	93.19 6.81 3.1×10^{-4}	98.81 1.19 2.9×10^{-4}	100	100	100	100	99.77 0.23
Mass proportions, %	2.6×10^{-4} 78.1 21.9	3.6 95.7 0.7	0.4 95.7 3.9	100	100	100	100	50 50
$\omega_{0.70}^A$	0.94	0.88	0.76	0.71	0.85	0.93	0.93	0.92
$\sigma_{0.55}^*$, $m^2\ g^{-1}$	0.82	0.42	0.12	0.03	0.23	0.77	0.80	0.578
α	0.3	0.0	0.0	- 0.1	- 0.1	0.6	- 0.2	- 0.1

The optical properties ($\omega_{0.70}^A$, the single-scattering albedo at $\bar{\lambda}$ = 0.70 μm; $\sigma_{0.55}^*$, the specific extinction cross section at 0.55 μm; α, the Angström exponent between 0.55 and 0.7 μm) of the different desert aerosol models were computed for a complex refractive index of 1.55 - i 0.005 and a volumic mass of 2.5 g cm^{-3}.

two models of desert dust in the Mediterranean (DM1 and DM2) come from desert aerosol sampling in Corsica, France. The monomodal model was derived from cascade impactor samples [*Dulac et al.*, 1992a], and the bimodal model resulted from dry deposition sampling [*Dulac et al.*, 1992b]. The various phase functions of these models are shown in Figure 6. This set of models seems well adapted to our sensitivity study because it enables us to explore a wide range of particle size distributions. However, among these models, only two have a phase function significantly lower than the phase function of the background desert aerosol model of Shettle, the wind-carrying dust model of *D'Almeida* [1987] and the near-source model of *Schütz* [1980]. These two models are characteristic of desert aerosol close to the source and give a strong importance to the large size fraction. Consequently, this confirms that only models with a dominant fraction of very large particles enable us to modify the phase function for a better fit between Meteosat- and Sun-photometer-derived aerosol optical thicknesses. However, the mass-particle size distributions of such models are definitely not coherent with observations of desert dust in marine areas.

Complex refractive index. We now examine the impact of the refractive index on optical properties of the background desert dust model (DD). The complex refractive index of a particle depends on its chemical composition: the real part n_{Re} characterizes the scattering properties of the medium; the imaginary part n_{Im} characterizes the absorption properties of the material. For atmospheric aerosols in the visible spectrum [*Jennings*, 1981] the real part ranges between 1.3 and 2.1 and the imaginary part between 0 and 0.8. Because of the difficulty of measurements, few data are available on desert aerosols real refractive index. Some workers [*Grams et al.*, 1974; *DeLuisi et al.*, 1976; *Patterson et al.*, 1977] found a typical range of 1.45-1.60 in the visible spectrum, but most of these authors recommend a "representative value" ranging from 1.50 to 1.55. The imaginary part is easier to estimate from attenuation measurements but also more variable, mainly because of the potential contamination of dust samples by absorbing aerosols of combustion origin [*Levin and Lindberg*, 1979]. *Grams et al.* [1974] found values between 0.003 and 0.015 at about 0.500 μm in a semi-arid region (Big Spring, Texas) and recommend a value of 0.005. *Patterson et al.* [1977] performed numerous measurements of the imaginary part of the refractive index of

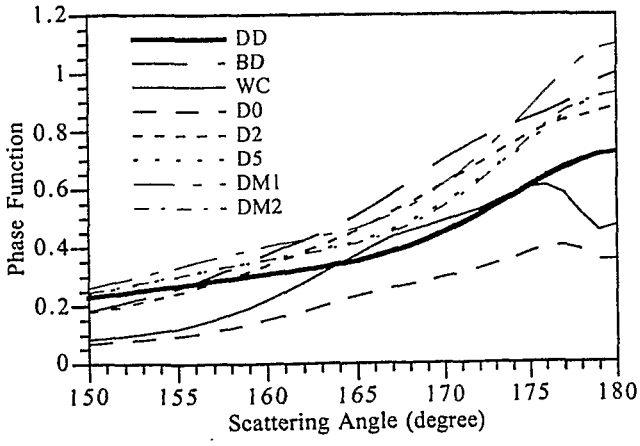

Figure 6. Phase functions at $\bar{\lambda}$ = 0.70 μm of the various desert aerosol models tested in this study. The different desert aerosol models are described in Table 3, and the phase functions were computed for a complex refractive index of 1.55 - *i* 0.005.

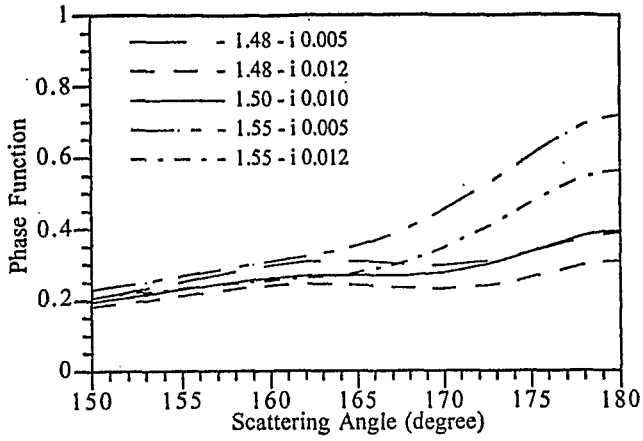

Figure 7. Phase function at $\bar{\lambda}$ = 0.70 μm of the *Shettle*'s [1984] background desert dust model (Table 3) for different refractive indices.

Saharan aerosols over the Atlantic during the Global Atmospheric Research Program Atlantic Tropical Experiment (GATE). They found a mean value of 0.008, but with a strong spectral dependence, between 0.025 at 0.3 μm and 0.004 at 0.7 μm. This may be a problem for Meteosat which has a wide spectral band (0.35 - 1.10 μm). However, *World Climate Program (WCP)* [1983] recommends a constant value of 1.53 - *i* 0.008 for the remote continental dust-like model over the whole Meteosat spectral band. In this work, we considered a spectrally constant value of the refractive index, and we performed Mie computations for realistic variations of the refractive index: n_{Re} = 1.48, 1.50, 1.53, 1.55; n_{Im} = 0.005, 0.008, 0.010, 0.012. Figure 7 shows that such variations may induce strong modifications of the phase function of the background desert dust model which might explain the bias observed between Sun photometer and Meteosat optical thickness at Meteosat scattering angles. In contrast, the single-scattering albedo exhibits only small variations (about 5%) for the different complex refractive indices.

3.3. Final Desert Aerosol Model

The previous tests showed that the size distribution of the *Shettle*'s [1984] model may be considered as representative of the desert aerosols transported over marine areas and that variations of the refractive index of these particles may strongly influence our Meteosat results. It suggested that the refractive index of 1.55 - *i* 0.005, which we initially used in our inversion as characteristic of the desert aerosols, may be the cause of the bias of about 30% with Sun photometer measurements. For the different refractive indices considered, we computed the aerosol optical properties and we performed the Meteosat inversion corresponding to each Sun photometer measurement (see Table 2). The slopes and correlation coefficients of the linear fit with Sun photometer data for each refractive index are shown in Table 4. The best correlation is obtained for a complex refractive index of 1.50 - *i* 0.010, with a slope of 1.04 ± 0.05 and a correlation coefficient of 0.97. Figure 8 compares the Meteosat and Sun photometer dust optical thicknesses for the initial refractive index of 1.55 - *i* 0.005 and for its most suitable value of 1.50 - *i* 0.010. Although the value of 0.01 for the imaginary part of the refractive index of desert particles may appear large compared to some other studies, it must be seen as an average value within the

Table 4. Slopes and Correlation Coefficients of the Linear Fit of the 24 Coincident Meteosat-Derived and Sun-Photometer-Derived Optical Thicknesses Shown in Table 2 for Various Real (n_{Re}) and Imaginary (n_{Im}) Parts of the Refractive Index

	n_{Re}			
n_{Im}	1.48	1.50	1.53	1.55
-*i* 0.005	0.90 ± 0.02 (0.97)	0.80 ± 0.03 (0.96)	0.67 ± 0.04 (0.95)	[0.60 ± 0.04 (0.94)]
-*i* 0.008	1.04 ± 0.02 (0.97)	0.92 ± 0.04 (0.96)	0.78 ± 0.05 (0.96)	0.69 ± 0.06 (0.94)
-*i* 0.010	1.12 ± 0.03 (0.97)	[1.04 ± 0.05 (0.97)]	0.85 ± 0.05 (0.96)	0.76 ± 0.06 (0.95)
-*i* 0.012	1.20 ± 0.03 (0.97)	1.09 ± 0.05 (0.97)	0.93 ± 0.06 (0.96)	0.83 ± 0.06 (0.95)

Correlation coefficients are given in parentheses. The two cases in brackets are plotted in Figure 8.

wide Meteosat VIS spectral band, and it appears consistent with the published results cited above. *Ignatov et al.* [1995] also found that such a refractive index of 1.50 - *i* 0.010 (at 0.63 μm) yield a perfect agreement between Sun photometer and operational Advanced Very High Resolution Radiometer (AVHRR) retrievals of the aerosol optical depth in the North Atlantic and Mediterranean Sea. In addition, the Angström exponent of 0.3 in the visible spectrum of this desert aerosol model is compatible with our Sun photometer measurements (Table 2) and is very close to the value of 0.35 recommended by *Cerf* [1980] for the tropical western Africa. This desert aerosol model was incorporated in the inversion procedure.

It is possible that within this wide range of wavelengths some biases compensate each other. For instance, we considered that all particles are spherical, a classical assumption which does not correspond to observations. The nonsphericity of mineral particles is recognized to have important consequences on their optical properties. *Koepke and Hess* [1988] considering ovoid particles, as well as *Mishchenko et al.* [1995] considering oblates and prolates, seem to agree on a general effect of nonsphericity toward a decrease of backscattering. This field of research is still wide open, and more work needs to be done on the actual shapes of mineral aerosol particles.

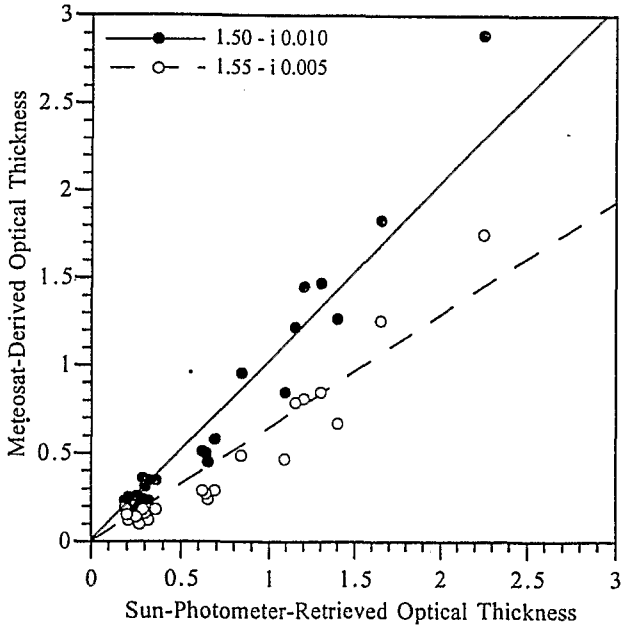

Figure 8. Comparison of Meteosat- and Sun-photometer-retrieved desert dust optical thickness for the first data set of sunphotometer measurements (Table 2), for two values of the refractive index, and for the DD size distribution model. The best agreement is obtained for a refractive index of 1.50 - *i* 0.010. Slopes and correlation coefficients are given in Table 4.

4. Validation of the Method

To achieve the validation of our algorithm, we need an independent set of data, which had not been used to constrain the desert aerosol model. We use the two months of automatic measurements at Sal Island in late 1994. These data are presented in Table 5, including the date and location as well as the aerosol optical thickness and Angström exponent of each measurement. Contrary to the first subset of data (Table 2) the Angström exponent sometimes goes above 0.5. Our method generally provides two types of information for a given site: for clear sky, Meteosat pixel is directly inverted to obtain the optical thickness; for cloudy conditions the desert dust field is interpolated from the closest available pixels. The validation of the inversion procedure is done only on clear sky pixels, but the uncertainty due to interpolation may be likewise shown by comparison with Sun photometers for cloudy conditions. To test the actual results of the Meteosat inversion, we do not apply the same criteria as in section 3.1 to select the Sun photometer measurements. As explained by *Moulin et al.* [this issue], the only selection criterion was to reject Sun photometer data when there were no clear sky Meteosat pixels closer than 200 km to the site (five data rejected). We analyzed the corresponding Meteosat 5 images using the background desert aerosol size distribution of *Shettle* [1984] and the new refractive index of 1.50 - *i* 0.010. The results are shown on Figure 9, where the solid circles represent clear sky pixels (quality of the inversion) and the open circles represent cloudy conditions (quality of the interpolation). The correlation between Meteosat- and Sun-photometer-derived optical thicknesses for clear sky pixels is 0.965, with a slope nonsignificantly different from 1.0. For the two subsets of Sun photometer data the maximum dispersion of Meteosat-derived desert dust optical thickness is 25% (Figures 8 and 9). This good agreement does not necessarily mean that each of our assumptions in the inversion procedure is correct, but it gives confidence that the final results can be trusted in a wide range of aerosol thicknesses. The interpolation yields a stronger dispersion: the values of dust optical thickness interpolated from clear sky pixels, when at least one is closer than 200 km from the site, are all within a factor of 2 from the Sun photometer data.

Table 5. Set of Sun Photometer Measurements Used for Validating the Meteosat-Based Estimation of the Aerosol Optical Thickness in 1994

Date	$\tau^A_{0.55}$	α	Date	$\tau^A_{0.55}$	α
October 22, 1994	0.13	0.14	November 22, 1994[a]	0.58	0.20
October 23, 1994	0.30	0.12	November 24, 1994	0.30	0.34
October 24, 1994[a]	0.20	0.20	November 25, 1994	0.16	0.24
October 26, 1994	0.19	0.13	November 27, 1994	0.12	0.20
October 27, 1994[a]	0.17	0.30	November 28, 1994[a]	0.16	1.20
October 28, 1994	0.10	0.28	November 30, 1994	0.36	0.10
October 30, 1994	0.10	0.28	December 1, 1994	0.12	0.50
October 31, 1994[a]	0.04	0.30	December 2, 1994[a]	0.09	0.60
November 1, 1994[a]	0.08	0.30	December 4, 1994	0.24	0.23
November 3, 1994[a]	0.08	0.40	December 5, 1994	0.45	0.05
November 5, 1994	0.61	0.10	December 6, 1994[a]	0.75	0.01
November 6, 1994	0.82	-.08	December 7, 1994[a]	0.54	0.10
November 7, 1994	0.70	0.25	December 8, 1994	0.48	0.07
November 9, 1994[a]	0.57	0.10	December 9, 1994[a]	0.90	0.10
November 10, 1994	0.36	0.30	December 10, 1994	0.59	0.17
November 11, 1994	0.32	0.21	December 11, 1994	0.40	0.33
November 12, 1994	0.28	0.30	December 12, 1994	0.40	0.30
November 13, 1994[a]	0.21	0.30	December 16, 1994[a]	0.39	0.50
November 14, 1994	0.28	0.21	December 21, 1994	0.16	0.46
November 15, 1994	0.21	0.17	December 27, 1994	0.45	0.17
November 17, 1994[a]	0.67	0.50	December 29, 1994	0.32	0.30
November 18, 1994	0.67	0.10	December 30, 1994[a]	0.38	0.50
November 19, 1994	0.55	0.10			

All measurements were performed at Sal Island (16.73°N, 22.95°W), Cape Verde. The corresponding Meteosat sensor is Meteosat 5.

[a]No Meteosat clear sky pixel available on the site. The Meteosat value will be interpolated if at least one clear sky pixel is closer than 200 km.

Consequently, we believe that they can be used to estimate the order of magnitude of dust transport over periods which would be too cloudy to allow any other information. A much larger data set would be needed for a statistical evaluation of the interpolated data set.

5. Major Causes of Uncertainty

Our determination of the desert dust optical thickness is only valid for situations close to the climatological conditions [*Moulin et al.*, this issue] for tropospheric and stratospheric sulphates. After a volcanic eruption or a strong pollution event, the optical thickness of nondesert aerosols may change within a few days and for specific regions. In such cases our automated treatment of the Meteosat data must be replaced by a case study using improved information on atmospheric aerosols. In this section we only examine the different uncertainties of the inversion procedure within the normal range of our algorithmic procedure. We discuss their effect on the determination of dust aerosol optical thickness. To achieve this, we performed sensitivity tests by modifying separately different parameters of the radiative transfer model 5S [*Tanré et al.*, 1990] used during our inversion procedure. We also discuss the uncertainties due to the various radiative transfer approximations of 5S itself.

5.1. Inversion Parameters

For the two sensors Meteosat 2 and 4 we tested the sensitivity of our inversion procedure to different parameters: calibration and radiometric accuracy of the sensor, phase function of the desert aerosol, and reflectance of the sea surface. We first list the major uncertainties and then comment on their consequences on dust aerosol determination.

The relative uncertainty on the calibration coefficient (a) is ±13% and the offset numeric count (NC_0) is given within ±1NC [*Moulin et al.*, 1996]. The uncertainty on the radiometric measurement is of ±2NC and ±0.5NC for Meteosat 2 and 4, respectively. The phase function and its uncertainty depend on the scattering angle. Assuming that the desert dust optical properties are now well known, we selected the phase functions of the five aerosol models in Table 4 which lead to a realistic comparison between Meteosat- and Sun-photometer-derived aerosol optical thickness, i.e., to a slope between 0.9 and 1.1. For a given scattering angle in the range of interest (150°-180°) the standard deviation of these phase functions may vary by ±3% at low scattering angles and ±13% at the largest angles (180°). The spectral sea surface reflectance is sensitive to the phytoplankton content and sea state, and we assumed [after *Moulin et al.*, 1996] a relative uncertainty of ±30% on the integrated sea surface reflectance.

For each parameter and for several sites in the Mediterranean Sea and in the Atlantic, we used 5S iteratively to estimate the uncertainty on $\tau^A_{0.55}$. We computed mean quadratic uncertainties by considering that the different parameters are independent. This theoretical uncertainty is maximum for low optical

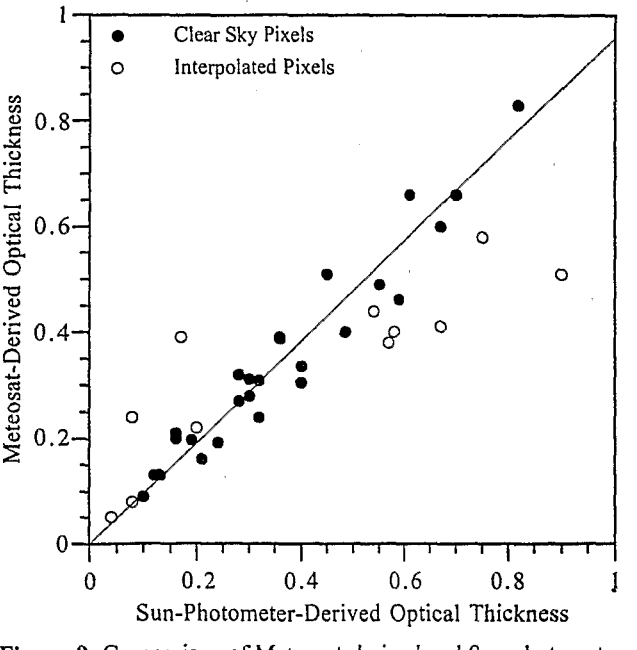

Figure 9. Comparison of Meteosat-derived and Sun-photometer-derived desert dust optical thickness for the, 1994 Sal data set (Table 5), using the new refractive index of 1.50 - i 0.010. The line is the best linear fit between Sun photometer values and clear sky Meteosat values. The slope is 0.96 ± 0.05, and the correlation coefficient is 0.965 for the 29 clear sky pixels. For the 16 other days the considered area was too cloudy to allow a fair comparison with Meteosat data. However, when the closest available pixel was distant by less than 200 km from our site, we show the interpolated values as open circles (11 data).

thicknesses (between ±65% and ±100% at 0.2) and strongly decreases to reach values between ±40% and ±50% for an optical thickness of 0.4. For higher optical thicknesses, it remains about constant with a mean value between ±30 and ±40%. Surprisingly, these results are not significantly different for Meteosat 2 and 4 despite the improvement of the Meteosat 4 digitization. Indeed, the accuracy of the calibration and of the digitization are found to be the main source of uncertainty for the retrieval of desert dust optical thickness from Meteosat data. The decrease of the uncertainty gained for Meteosat 4 digitization is then compensated by the increase of uncertainty on the calibration. For a desert dust optical thickness of 0.4 the calibration and digitization contributes to 75-85% of the overall uncertainty on Meteosat 2 estimates, whereas for Meteosat 4 the calibration alone contributes to 70-80% of the overall uncertainty. This result stresses the need for accurate calibration of space sensors for quantitative aerosol studies.

5.2. Radiative Transfer Model Approximations

Another source of error comes from the various approximations used in 5S to compute aerosol optical thickness from the simulated satellite radiance. We estimated this error by comparing the satellite signal computed with 5S and with an improved version named 6S (second simulation of the satellite signal in the solar spectrum) developed more recently [*Vermote et al.*, 1994]. Compared with 5S, the radiative transfer model 6S enables the computation of (1) a more accurate gaseous transmission by taking into account new coefficients, based on HITRAN 91 values [*Rothmanet al.*, 1992], for the absorbing gases (H_2O, O_3, O_2, and CO_2) contributions; (2) more accurate Rayleigh and aerosol reflectances and transmissions by using updated approximations and successive orders of scattering method in a discrete atmosphere; and (3) an improved spectral integration with a step of 2.5 nm instead of the 5S resolution of 5 nm. The differences between 5S and 6S strongly depend on the geometry of the measurement and on the aerosol optical thickness. In some cases such as for large dust loads, the difference in $\tau_{0.55}^{A}$ may reach ±40%, but on the average, for our Meteosat observation conditions the discrepancy is of the order of ±15% for a dust optical thickness of 0.4. This result shows that in the majority of cases the radiative transfer model approximations do not constitute the main source of error.

6. Conclusion

The validation of our method to retrieve desert dust optical thickness over seawater from Meteosat data has been made by comparison with Sun photometer data. We first observed that our Meteosat results were underestimated by about 40%. We showed that only the properties of the desert aerosol model [*Shettle*, 1984] could be responsible for this discrepancy. The size distribution of mineral particles could not account for the observed effect, but a modification of their refractive index within a realistic range (1.50 - *i* 0.010) gave satisfactory results. A lot of effort has been devoted to define average optical properties which are realistic over the wide spectrum of the Meteosat VIS channel. This paper stresses the interest of complementing satellite data by Sun photometer network information. The performed testing gives confidence that our Meteosat data set, which covers five different sensors with various spectral bands and radiometric sensitivities, is internally consistent. The accuracy of the retrievals greatly depends on an accurate calibration of the sensor. The comparison of Meteosat-derived estimates of the desert aerosol optical thickness with independent Sun photometer measurements exhibits a maximum dispersion of 25%. This general estimate of accuracy does not apply to values interpolated under water clouds. The relevance of our interpolation clearly depends on the dispersion of valid dust data points as well as on the relative extension of water clouds and dust plumes, but it should be noticed that this error decreases when dealing with time-averaged images for climatological purposes. The validity of our interpolation procedure was assessed from a comparison between an independent set of Sun photometer data and the interpolated value in cloudy pixels. The agreement is within a factor of 2 of Sun photometer data when at least one of the clear sky pixels used for interpolation was located at less than 200 km (six pixels) from the site.

Acknowledgments. A great number of persons contributed to the Sun photometer original data set presented here. First, we are grateful to L. Méninger, Laboratoire de Météorologie Dynamique, for the development of the portable instrument and for measurements in Corsica. C. Devaux, Laboratoire d'Optique Atmosphérique, is acknowledged for kindly providing us with his Sun photometer data from Senegal. H. Cachier is also acknowledged for her conscientious Sun photometer measurements during the EUMELI 3 cruise. Initial help from L. Méninger and D. Tanré in Sun photometer data analysis was appreciated. We are particularly grateful to O. Silva and M. Santos Soares, successive directors of the Cape Verde Meteorological Service, who welcomed us and made the measurements possible at Sal Island. We are also indebted to G. Bergametti for his organization of in situ aerosol measurement campaigns in Corsica and Sal Island and his friendly participation to Sun photometer measurements. M. I. Mishchenko has genereously provided us with a code to test particle nonsphericity implications. This work is part of a close collaboration between the LMCE and the CFR and was supported by the French Commissariat à l'Energie Atomique (CEA) and the Centre National de la Recherche Scientifique (CNRS). Additional support was provided by INSU/CNRS and the French Ministère de l'Environnement first through the "ATP Aérosols Désertiques" and then through the research project "Erosion Eolienne en Régions Arides et Semi-Arides" of the "Programme Environnement/section Phase Atmosphérique des Grands Cycles Biogéochimiques". C. E. Lambert and F. Dulac would like to express their gratitude to the CEA for the computing facilities and the generous hospitality provided by the LMCE. Authors acknowledge the two anonymous reviewers of the paper for valuable comments. This is CFR contribution 1871 and LMCE contribution 379.

References

Angström, A., The parameters of atmospheric turbidity, *Tellus*, *16*, 64-75, 1964.

Balkanski, Y., M. Schulz, B. Marticorena, G. Bergametti, W. Guelle, F. Dulac, C. Moulin, and C. E. Lambert, Importance of the source term and of the size distribution to model the mineral dust cycle, in *The Impact of Desert Dust Across the Mediterranean*, edited by S. Guerzoni and R. Chester, pp. 69-76, Kluwer Acad., Norwell, Mass., 1996.

Ben Mohamed, A., J.-P. Frangi, J. Fontan, and A. Druilhet, Spatial and temporal variations of atmospheric turbidity and related parameters in Niger, *J. Appl. Meteorol.*, *31*, 1286-1294, 1992.

Bergametti, G., Apports de matière par voie atmosphérique à la Méditerranée occidentale: Aspects géochimiques et météorologiques, Ph.D. thesis, Univ. of Paris 7, 1987.

Bergametti, G., A.-L. Dutot, P. Buat-Ménard, R. Losno, and E. Remoudaki, Seasonal variability of the elemental composition of atmospheric aerosol particles over the northwestern Mediterranean, *Tellus, Ser. B.*, *41*, 353-361, 1989.

Carlson, T. N., and R. S. Caverly, Radiative characteristics of Saharan dust at solar wavelengths, *J. Geophys. Res.*, *82*, 3141-3152, 1977.

Cerf, A., Atmospheric turbidity over west Africa, *Contrib. Atmos. Phys.*, *53*, 414-429, 1980.

Chazette, P., C. David, J. Lefrère, S. Godin, J. Pelon, and G. Mégie, Comparative lidar study of the optical, geometrical, and dynamical properties of stratospheric postvolcanic aerosols, following the eruptions of El Chichon and Mount Pinatubo, *J. Geophys. Res.*, *100*, 23,195-23,207, 1995.

Chiapello, I., G. Bergametti, L. Gomes, B. Chatenet, F. Dulac, J. Pimenta, and E. Santos Suares, An additional low layer transport of Sahelian and Saharan dust over the north-eastern tropical Atlantic, *Geophys. Res. Lett.*, *22*(23), 3191-3194, 1995.

D'Almeida, G. A., On the variability of desert aerosol radiative characteristics, *J. Geophys. Res.*, *92*, 3017-3026, 1987.

DeLuisi, J. J., P. M. Furukawa, D. A. Gillette, B. G. Schuster, R. J. Charlson, W. M. Porch, B. M. Herman, R. A. Rabinoff, J. T. Twitty, and J. A. Weinman, Results of a comprehensive atmospheric aerosol-radiation experiment in the southwestern United States, II: Radiation flux measurements and theoretical interpretation, *J. Appl. Meteorol.*, *15*, 455-463, 1976.

Dulac, F., P. Buat-Ménard, U. Ezat, S. Melki, and G. Bergametti, Atmospheric input of trace metals to the western Mediterranean: Uncertainties in modelling dry deposition from cascade impactor data, *Tellus, Ser. B.*, *41*, 362-378, 1989.

Dulac, F., D. Tanré, G. Bergametti, P. Buat-Ménard, M. Desbois And D. Sutton, Assessment of the African airborne dust mass over the Mediterranean sea using Meteosat data, *J. Geophys. Res.*, *97*, 2489-2506, 1992a.

Dulac, F., G. Bergametti, R. Losno, E. Remoudaki, L. Gomes, U. Ezat, and P. Buat-Ménard, Dry deposition of mineral aerosol particles in the atmosphere: significance of the large size fraction, in *Precipitation Scavenging and Atmosphere-Surface exchange*, vol. 2, edited by S. E. Schwartz and W. G. N. Slinn, pp. 841-854, Hemisphere, Bristol, Pa., 1992b.

Fouquart, Y., B. Bonnel, M. Chaoui Roquai, R. Santer, and A. Cerf, Observations of Saharan aerosols: Results of ECLATS field experiment, I: Optical thicknesses and aerosol size distribution, *J. Clim. Appl. Meteorol.*, *26*, 28-37 1987.

Grams, G. W., I. H. Blifford Jr., D. A. Gillette, and P. B. Russell, Complex index of refraction of airborne soil particles, *J. Appl. Meteorol.*, *13*, 459-471, 1974.

Griggs, M., Satellite measurements of tropospheric aerosols, *Adv. Space Res.*, *2*, 109-118, 1983.

Holben, B.N., T.F. Eck, and R. S. Fraser, Temporal and spatial variability of aerosol optical depth in the Sahel region in relation to vegetation remote sensing, *Int. J. Remote Sens.*, *12*(6), 1147-1163, 1991.

Holben, B.N., et al., Multiband automatic sun and sky scanning radiometer system for measurements of aerosols, *Remote. Sens. Environ.*, in press, 1996.

Hoppel, W. A., J. W. Fitzgerald, G. M. Frick, R. E. Larson, and E. J. Mack, Aerosol size distributions and optical properties found in the marine boundary layer over the Atlantic Ocean, *J. Geophys. Res.*, *95*, 3659-3686, 1990.

Ignatov, A. M., L. L. Stowe, S. M. Sakerin, and G. K. Korotaev, Validation of the NOAA/NESDIS satellite aerosol product over the North Atlantic in 1989, *J. Geophys. Res.*, *100*, 5123-5132, 1995.

Jäger, H., O. Uchino, T. Nagai, T. Fujimoto, V. Freudenthaler, and F. Homburg, Ground-based remote sensing of the decaying of the Pinatubo eruption cloud at 3 northern hemisphere sites, *Geophys. Res. Lett.*, *22*(5), 607-610, 1995.

Jankowiak, I., and D. Tanré, Satellite climatology of Saharan dust outbreaks: method and preliminary results, *J. Clim.*, *5*, 646-656, 1992.

Jennings, S. G., The effect of particle size distribution and complex index of refraction of atmospheric aerosols on the visual range, in *Atmospheric Aerosols and Nuclei*, edited by Roddy and O'Connor, pp. 415-420, 1981.

Junge, C. E., *Air Chemistry and Radioactivity*, edited by J. Van Mieghem, Academic, San Diego, Calif., 1963.

Koepke, P., Calibration of the VIS-channel of Meteosat-2, *Adv. Space Res.*, *2*, 93-96, 1983.

Koepke, P., and M. Hess, Scattering functions of tropospheric aerosols: The effects of nonspherical particles, *Appl. Opt.*, *27*(12), 2422-2430, 1988.

Lauleinen, N. S., A. J. Alkezweeny, and J. M. Thorp, Simultaneous aerosol size distribution and turbidity measurements over Saint-Louis during METROMEX 1975, *J. Appl. Meteorol.*, *17*, 615-626, 1978.

Levin, Z., and J. D. Lindberg, Size distribution, chemical composition, and optical properties of urban and desert aerosols in Israel, *J. Geophys. Res.*, *84*, 6941-6950, 1979.

Liousse, C., C. Devaux, F. Dulac, H. Cachier, Aging of savanna biomass burning aerosols: Consequences on their optical properties, *J. Atmos. Chem.*, *22*, 1-17.

Mc Clatchey, R. A., R. W. Fenn, J. E. A. Selby, F. E. Volz, and J. S. Garing, Optical properties of the atmosphere, *Rep. AFCRL-TR-71-0279, Environ. Res. Pap. 354*, Air Force Cambridge Res. Lab., Bedford, Mass., 1971.

Mishchenko, M. I., A. A. Lacis, B. E. Carlson, and L. D. Travis, Nonsphericity of dust-like tropospheric aerosols: Implications for remote sensing and climate modeling, *Geophys. Res. Lett.*, *22*(9), 1077-1080, 1995.

Moulin, C., C. E. Lambert, J. Poitou, and F. Dulac, Long-term (1983-1994) calibration of the Meteosat solar (VIS) channel using desert and marine targets, *Int. J. Remote Sens.*, *17*(6), 1183-1200, 1996.

Moulin, C., F. Guillard, F. Dulac, and C. E. Lambert, Long-term daily monitoring of Saharan dust load over marine areas using Meteosat ISCCP-B2 data, 1, Methodology and preliminary results for 1983-1994 in the western Mediterranean, *J. Geophys. Res.*, this issue.

Patterson, E. M., D. A. Gillette, and B. H. Stockton, Complex index of refraction between 300 and 700 nm for Saharan aerosols, *J. Geophys. Res.*, *82*, 3153-3160, 1977.

Putaud, J.-P., S. Belviso, B. C. Nguyen, and N. Mihalopoulos, Dimethylsulfide, aerosols and condensation nuclei over the tropical northeastern Atlantic Ocean, *J. Geophys. Res.*, *98*, 14,863-14,871, 1993.

Rothman, L. S., et al., The HITRAN molecular data base: Editions of 1991 and 1992, *J. Quant. Spectrosc. Radiat. Transfer*, *48*, 469-507, 1992.

Schütz, L., Long range transport of desert dust with special emphasis on the Sahara, *Ann. N. Y. Acad. Sci.*, *338*, 15-20, 1980.

Shettle, E. P., Optical and radiative properties of a desert aerosol model, in *Proceedings of the Symposium on Radiation in the Atmosphere*, edited by G. Fiocco, pp. 74-77, A. Deepak, Hampton, Va., 1984.

Tanré, D., C. Devaux, M. Herman, R. Santer, and Y. Gac, Radiative properties of desert aerosols by optical ground-based measurements at solar wavelengths, *J. Geophys. Res.*, *93*, 14,223-14,231, 1988.

Tanré, D., C. Derro, P. Duhaut, M. Herman, J. J. Morcrette, J. Perbos, and P. Y. Deschamps, Description of a computer code to simulate the satellite in the solar spectrum: The 5S code, *Int. J. Remote Sens.*, *11*, 659-668, 1990.

Tomasi, C., and F. Prodi, Measurements of atmospheric turbidity and vertical mass loading of particulate matter in marine environments (Red Sea, Indian Ocean, and Somalian coast), *J. Geophys. Res.*, *87*, 1279-1286, 1982.

Tomasi, C., F. Prodi, and F. Tampieri, Atmospheric turbidity variations caused by layers of Sahara dust particles, *Contrib. Atmos. Phys.*, *52*(3), 215-227, 1979.

Vermote, E., D. Tanré, J. L. Deuzé, M. Herman, and J. J. Morcrette, Second Simulation of the Satellite Signal in the Solar Spectrum (6S), *6S User Guide Version 0*, 1994.

World Climate Programme (WCP), Aerosols and Their Climatic Effects, *Ser. Rep. 55*, edited by A. Deepak and H. E. Gerber, Int. Counc. Sci. Unions and World Meteorol. Organ., Geneva, 1983.

P. Chazette and C. Moulin (corresponding author), Laboratoire de Modélisation du Climat et de l'Environnement, Commissariat à l'Energie Atomique, Centre d'études de Saclay, l'Orme des Merisiers, F-91191 Gif sur Yvette, France. (e-mail: chazette@cea.fr; cyril.moulin@cea.fr)

F. Dulac and C.E. Lambert, Centre des Faibles Radioactivités, Centre National de la Recherche Scientifique - Commissariat à l'Energie Atomique, F-91198 Gif-Sur-Yvette, France. (e-mail: dulac@cea.fr; lambertc@prolix.saclay.cea.fr)

I. Jankowiak, Laboratoire d'Optique Atmosphérique, Université des Sciences et Techniques de Lille - Centre National de la Recherche Scientifique, F-59655 Villeneuve d'Ascq, France. (e-mail: isabelle.jankowiak@univ-lille1.fr)

B. Chatenet, Laboratoire Interuniversitaire des Sytèmes Atmosphériques, Universités de Paris 7 and Paris 12 - Centre National de la Recherche Scientifique, F-94010 Créteil, France. (e-mail: chatenet@univ-paris12.fr)

F. Lavenu, Institut Français de Recherche Scientifique pour le Développement en Coopération, BP 182, Ouagadougou, Burkina Faso.

(Received February 29, 1996; revised August 1, 1996;
accepted August 7, 1996.)